Journal of Materials Chemistry C

Accepted Manuscript

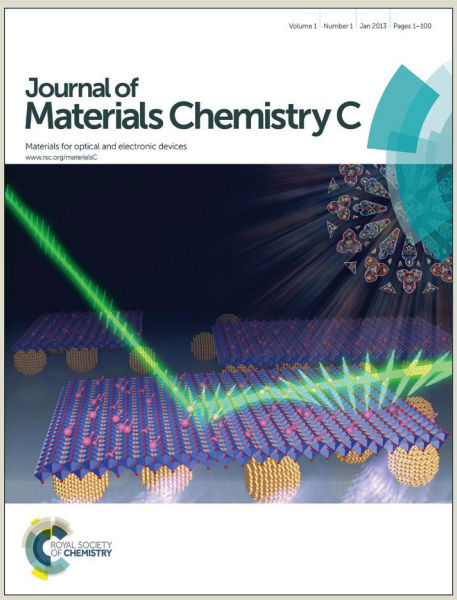

ROYAL SOCIETY OF CHEMISTRY

www.rsc.org/materialsC

Cite this: DOI: 10.1039/c0xx00000x

www.rsc.org/xxxxxx

ARTICLE TYPE

Spray coated ultrathin films from aqueous tungsten molybdenum oxide nanoparticle ink for high contrast electrochromic application

Haizeng Li,[a,b] Jingwei Chen,[b] Mengqi Cui,[b] Guofa Cai,[b] Alice Lee-Sie Eh,[b] Pooi See Lee,*[b] Hongzhi Wang,*[a] Qinghong Zhang[c] and Yaogang Li*[c]

Received (in XXX, XXX) Xth XXXXXXXXX 20XX, Accepted Xth XXXXXXXXX 20XX

DOI: 10.1039/b000000x

Ultrathin tungsten molybdenum oxide nanoparticle films were fabricated from aqueous ink by spray coating technique. With the in situ heating of the hot plate during spray coating process, the detrimental effects of oxygen vacancies on electrochromic (EC) materials could be eliminated. The spray coated ultrathin films exhibit higher contrast than the drop casted films, which would provide a versatile and promising platform for energy-saving smart (ESS) windows, batteries, and other applications.

Assembly technologies would substantially affect the physicochemical properties and, ultimately, the performance of thin films.[1] Thus, the development of compliant fabrication of films is critical to the emerging electronics technology. Recently, EC devices have attracted increased attention due to its capability of tuning down energy consumption with its application in ESS windows. Therefore, a lot of research has been actively explored to obtain high performance EC films through various methods, including Langmuir−Blodgett technique,[2] filtration,[3] spin coating,[4,5] layer-by-layer deposition,[6,7] electrodeposition,[8] anodic growth method,[9-11] hydrothermal techniques,[12-14] and drop casting.[15,16] However, each of these methods mentioned above has one or more characteristic drawbacks, including complicated process and high energy consumption, leading to the inconvenience of large area fabrication. The spray process has been proven to be a versatile and facile method to fabricate electrodes, which is considered to be one of the most promising film fabrication techniques. This is widely applied because the spray process can be done at high production speed and is compatible with large-scale electrode fabrication.[17,18]

Recently, molybdenum doped tungsten oxide has attracted much attention because it could exhibit a broadened optical absorption band.[19,20] Besides, higher electrochromic efficiencies are expected as a result of enhanced electron intervalence transfer between Mo^{5+} and W^{6+} states, in addition to Mo^{5+}, Mo^{6+} and W^{5+}, W^{6+} transitions.[21,22] Thus, spray coating technique was utilized to prepare molybdenum doped tungsten oxide films due to their enhanced EC performance.[23,24] However, the few reports regarding spray coated molybdenum doped tungsten oxide films had paid too much attention to the molecular precursors and finally the films were of bulk structure, which would greatly increase the diffusion paths of lithium ions in the active materials. To solve the issues, it is attractive to spray pre-formed tungsten molybdenum oxide nanoparticle ink, which could produce nanoparticle films and thus greatly shorten the diffusion paths of lithium ions in the EC materials and facilitate intimate contacts between EC materials and electrolyte/current collector. The investigation in spray coating pre-formed tungsten molybdenum oxide provides potential insights on ion transport mechanism and needs to be actively explored.

In this study, we firstly designed a facile chemical method to synthesize doped tungsten oxide nanoparticles with ultrasmall sizes by adding MoO_3 in a typical synthesis procedure of pure tungsten oxide. In the typical synthesis of pure tungsten oxide, hydrated tungsten oxide was prepared via hydrothermal method (see the experimental section). Fig. 1 (a) shows the X-ray powder diffraction (XRD) pattern of the pure hydrated tungsten oxide powder. All peaks of the as-prepared powder can be well indexed to the orthorhombic phase of $WO_3 \cdot 0.33H_2O$ (JCPDS Card No. 54-1012). FE-SEM picture (Fig. 1 (b)) shows that the sample has clusters structure composed of nanoplates with thickness about 30 nm. The formation of the nanoplates could be attributed to the natural layered structure of the hydrated tungsten oxide[25] and the presence of ethylene glycol (EG) as explained in our previous report.[12] The average size of the nanoplate clusters is estimated to be 1 μm, which would increase the diffusion paths of intercalation ions in the solid phase and thus leading to a slow response. Moreover, the big sizes of the nanoplate clusters make it difficult to get uniform ink and films. As mentioned above, the doping with molybdenum will not only improve the EC performance, but also increase the crystalline disorder and affect the grain growth.[19-24] In this case, molybdenum oxide was utilized to obtain doped tungsten oxide with smaller dimensions under same hydrothermal conditions. Thus, the desired nanoparticulate tungsten molybdenum oxide can be synthesized via this novel and facile wet chemical doping method. Fig. 1 (c) shows the XRD pattern of the as-synthesized powder. The optical photo of the as-prepared powder showing dark blue color, which suggests the nonstoichiometric nature of the material and the existence of oxygen vacancies.[4,26-28] From the XRD pattern, it is confirmed that the as-synthesized powder is tungsten molybdenum oxide ($W_{0.71}Mo_{0.29}O_{3-x}$) with monoclinic phase. The obvious broadened reflection peaks imply smaller crystalline sizes of the particles. FE-SEM image (Fig. 1(d)) shows that the nanoplate clusters could be changed to nanoparticles after the addition of MoO_3 with a drastic reduction in clusters size, in agreement to the XRD result. The

TEM image (Fig. 1(e)) of the tungsten molybdenum oxide reveals that the nanoparticles with nearly spherical shapes possess an average diameter of 20 nm. The distances between the adjacent lattice fringes were measured to be 0.31 and 0.253 nm, corresponding to the lattice spacing of (-112) and (-212) planes. As shown in the inset of Fig. 1 (e), the uniform ink exhibits a pale-blue color, which is typically related with presence of oxygen vacancies.[4,26-28]

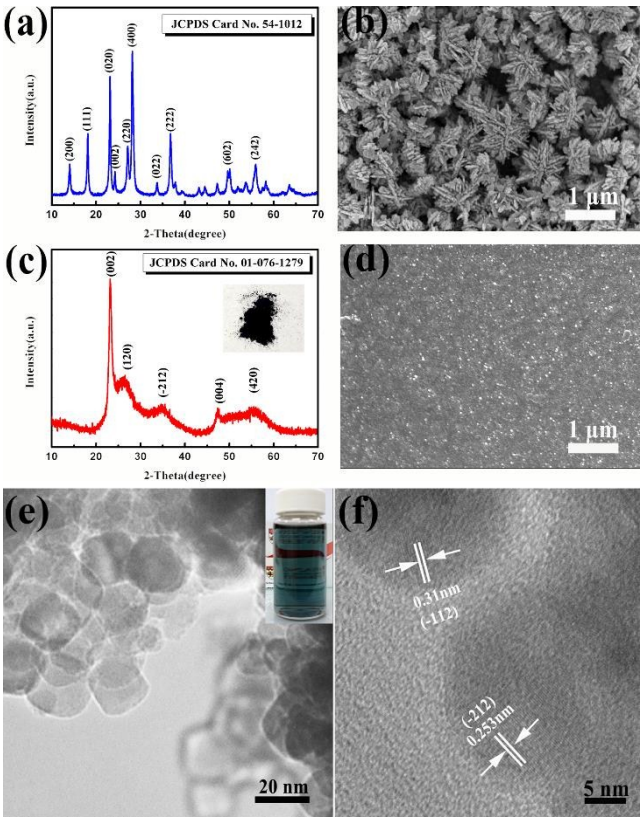

Fig. 1 (a) XRD pattern of as-prepared pure hydrated tungsten oxide. (b) FE-SEM images of as-prepared hydrated tungsten oxide powder. (c) XRD pattern of as-prepared tungsten molybdenum oxide. (d) FE-SEM image of as-prepared tungsten molybdenum oxide powder. (e) Low-magnification and (f) high-resolution TEM images of as-prepared tungsten oxide materials confirming the successful achievement of $W_{0.71}Mo_{0.29}O_{3-x}$ nanoparticles with average sizes of 20 nm. Inset in (e), an optical photo of the dispersion in DI water showing pale-blue color, which suggests the existence of oxygen vacancies.

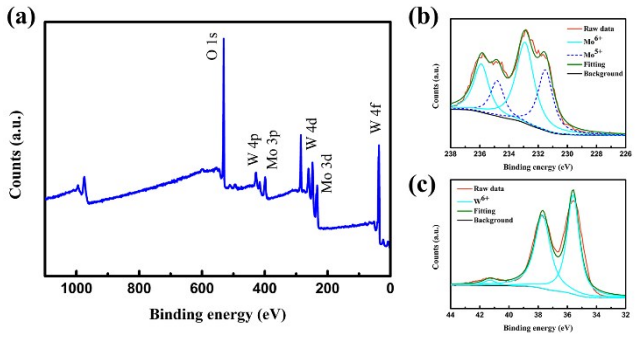

Fig. 2 (a) XPS survey spectra of tungsten molybdenum oxide nanoparticles. (b) Mo 3d XPS spectra. (c) W 4f XPS spectra.

In addition to XRD and TEM analysis, X-ray photoelectron spectroscopy (XPS) is used to identify the stoichiometry of the doped nanoparticles as shown in Fig. 2. The XPS survey spectra shown in Fig. 2 (a) indicates that the elements W, Mo, O exist in tungsten molybdenum oxide nanoparticles without other impurities. Corresponding high-resolution Mo 3d and W 4f XPS spectrum are used to identify the stoichiometry of the doped nanoparticles and shown in Fig. 2 (b and c). From Mo 3d XPS spectra (Fig. 2b), it is found that Mo^{6+} and Mo^{5+} ions coexist in the nanoparticles. The Mo^{5+} peaks (centered at 234.8 and 231.6 eV) are as obvious as the Mo^{6+} peaks (centered at 236.1 and 232.9 eV), suggesting a significant sub-stoichiometry for the doped nanoparticles. The W 4f XPS core-level spectra of the nanoparticles exhibits three peaks corresponding to W $4f_{7/2}$, W $4f_{5/2}$ and W $5p_{3/2}$, which are located at 35.5 eV, 37.7 eV and 41.3 eV, indicating that W in the doped nanoparticles is at the highest oxidation state (W^{6+}). These results reveal that Mo was introduced into the WO_3 lattice accompanied with the emergence of oxygen vacancies. The introduced Mo in WO_3 lattice will highly increase the structure disorder, which could prevent the preferred orientation growth and thus nanoparticles with small sizes could be prepared.

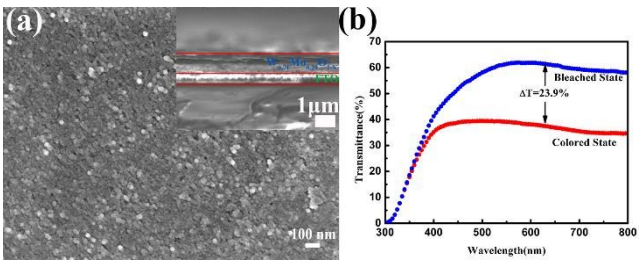

Fig. 3 (a) FE-SEM images of the drop casted tungsten molybdenum oxide film. The inset shows the cross-sectional view of the film. (b) UV-vis transmittance spectra of the drop casted film measured at −1.0 and +1.0 V, respectively.

To investigate the electrochromic performance of the as-prepared $W_{0.71}Mo_{0.29}O_{3-x}$ nanoparticles, the pale-blue ink was drop casted on FTO glass to form the EC film with a thickness of around 1 μm (see Fig. 3 (a)). Due to the detrimental effects of oxygen vacancies in EC materials,[29] the drop casted film shows a low modulation range (23.9%) even though there is a lot of active materials on the film. To eliminate the detrimental effects of oxygen vacancies, a facile in-situ oxidization with heating of the hot plate during spray coating process was utilized as the scheme illustrated in Fig. 4 (a) and (b). An ink containing $W_{0.71}Mo_{0.29}O_{3-x}$ nanoparticles is deposited as a continuous film on a FTO glass using spray coating technique (Fig. 4 (a)). Subsequent removal of DI water and in-situ oxidization with heating of the hot plate could induce the self-assembly of the $W_{0.71}Mo_{0.29}O_3$ film (Fig. 4 (b)), the pale yellow film and Mo 3d XPS spectrum of spray coated film and drop casted film reveal that the oxygen vacancies have been eliminated (see Fig. S1 and S2 in ESI). Fig. 4 (c) and (d) exhibit the surface morphology and cross-sectional view of the as-prepared spray coated $W_{0.71}Mo_{0.29}O_3$ film. $W_{0.71}Mo_{0.29}O_3$ nanoparticles are clearly seen with porous structures. The cross-section image (Inset in Fig. 4 (c)) shows that the thickness of the as-prepared spray coated $W_{0.71}Mo_{0.29}O_3$ film is around 200 nm, which is obviously thinner than that of drop casted film (which is around 1 μm) and previous reports.[11,12] The surface roughness of the film is also shown in Fig.

4, with amplitude of 60 nm for the region investigated. EDS (Energy Dispersive Spectroscopy) mapping of molybdenum and tungsten atoms was conducted and shown in Fig. S3. The uniform signal coverage of the elements across the selected area confirms that the spray coated film consists of tungsten molybdenum oxide.

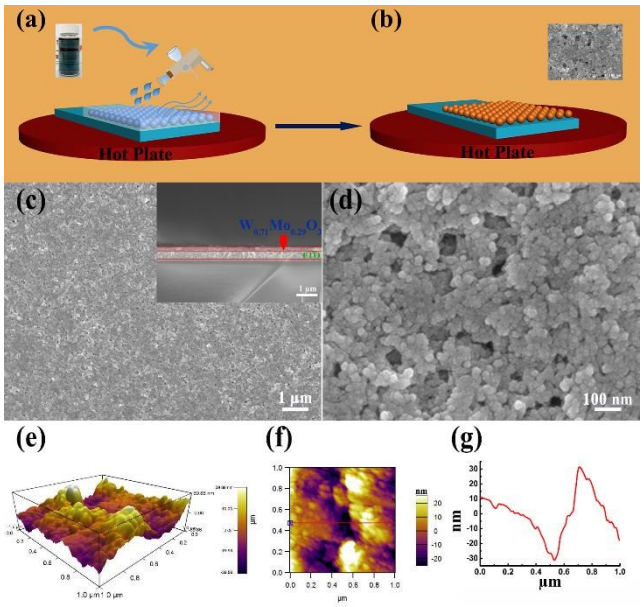

Fig. 4 (a) Pale blue solution is sprayed onto a FTO glass. (b) Coated substrate is dried and oxidized subsequently as the droplet sprayed onto the hot FTO glass. FE-SEM images the spray coated $W_{0.71}Mo_{0.29}O_3$ film: (c) low magnification, (d) higher magnification. The inset shows the cross-sectional view of $W_{0.71}Mo_{0.29}O_3$ film. (e-g) AFM images and rugosity measurements of the as-prepared spray coated $W_{0.71}Mo_{0.29}O_3$ film.

The EC phenomena of the spray coated $W_{0.71}Mo_{0.29}O_3$ film was investigated via an optical modulation test and characterization results were shown in Fig. 5 (a). The digital photographs shown in Fig. 5 (a) reveal that the logo placed below the film can be seen clearly, indicating fairly good transmittance of the film. The UV-vis transmittance spectra of the spray coated $W_{0.71}Mo_{0.29}O_3$ film in the colored and bleached states were measured at -1.0 V and +1.0 V, respectively (Fig. 5 (a)). The transmittance of the spray coated $W_{0.71}Mo_{0.29}O_3$ film at 632.8 nm is measured to be about 80% when bleached, which is much higher than that of the drop casted film (Fig. 3 (b)) and our previous reports.[12,13,30,31] In addition to the high transmittance of the bleached state, the spray coated $W_{0.71}Mo_{0.29}O_3$ film also has a high contrast when colored at a low voltage. The contrast of the spray coated $W_{0.71}Mo_{0.29}O_3$ film at 632.8 nm after applying voltage of -1.0 V is calculated to be 42.9 %, which is much higher than that of the drop casted film (Fig. 3 (b)) and previous reports.[31-33] To quantify the EC performance, contrast density is defined as the contrast provided by per unit film thickness. It has been calculated for drop casted film and spray coated film using the following Equation:

$$\text{Contrast density} = (T_{bleach} - T_{color})/D, \quad (1)$$

where D is the thickness of the film. As shown in Fig. 5 (b), the contrast density of spray coated $W_{0.71}Mo_{0.29}O_3$ film is about 10 times of that of the drop casted $W_{0.71}Mo_{0.29}O_{3-x}$ film. Besides, the contrast density of spray coated film is also fairly good than that calculated from our previous report (see Fig. S4 in ESI).[12] This high contrast density can be attributed to the elimination of oxygen vacancies and the increased electron transitions between two types of metallic sites in the molybdenum doped tungsten oxide.

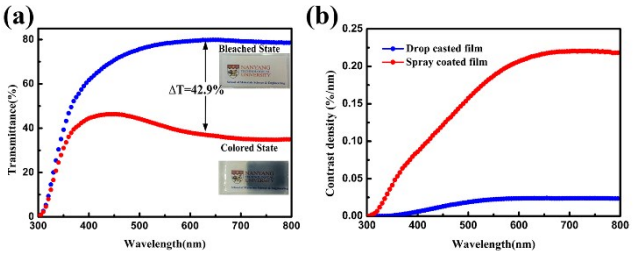

Fig. 5 (a) UV-vis transmittance spectra of the spray coated $W_{0.71}Mo_{0.29}O_3$ film at its colored and bleached state. (b) Contrast density of the spray coated film and drop casted film.

The assessment of the coloration–bleaching kinetics are vital for the evaluation of optical and electronic properties of the EC films.[34] Therefore, in situ normalized transmittance changes measured at an optical wavelength of 632.8 nm were measured using the chronoamperometric (CA) technique (Fig. 6). The coloration and bleaching times are always defined as the time taken to reach 90% of the optical modulation at 632.8 nm wavelength.[35,36] Fig. 6 shows the dynamic coloration/bleaching switching time for the drop casted $W_{0.71}Mo_{0.29}O_{3-x}$ film and spray coated $W_{0.71}Mo_{0.29}O_3$ film. For the drop casted film, the coloration time t_c and bleaching time t_b are found to be 5.5 and 7 s, respectively. Meanwhile, for the spray coated film, the coloration time t_c and bleaching time t_b are found to be 10 and 7.5 s, respectively. The response times of both films are all much faster than those of previous reports on pure tungsten oxide nanostructures.[12,13,37-39] Electrochemical impedance spectroscopy (EIS) measurements were conducted to investigate the intrinsic reason about spray coated film exhibiting longer responsive times than drop casted film. The Nyquist plots of both spray coated and drop casted films are shown in Fig. 6 (b). The high-frequency arcs corresponds to the charge-transfer impedance on the electrode/electrolyte surface. The semicircle of spray coated film is similar to that of drop casted film, indicating the similar charge-transfer resistance. The inclined line in low frequency is related to the ion diffusion process. The line of spray coated film exhibits a larger slope, suggesting its faster ion-diffusion process. These results demonstrate that the spray coated film possess fast ion diffusion, the longer responsive times of the spray coated film than that of the drop casted film can be attributed to the larger transmittance variation.

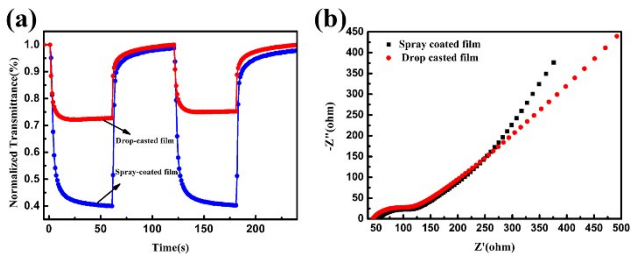

Fig. 6 (a) In situ normalized transmittance for the spray coated film and drop casted film at ±1V applied potentials for the optical wavelength of 632.8nm. (b) Nyquist plots of the spray coated film and drop casted film.

Coloration efficiency (CE), which is defined as the following

formulas:

$$CE = \Delta OD/(Q/A) \quad (2)$$

$$\Delta OD = \log(T_b/T_c) \quad (3)$$

where T_b and T_c refer to the transmittances of the film in its bleached and colored states, respectively. The calculated CE of the spray coated $W_{0.71}Mo_{0.29}O_3$ film is 36.3 $cm^2 C^{-1}$ at the wavelength of 632.8 nm (see Fig. S5 in ESI), which is comparable to other crystalline tungsten oxide.[8,10,32,38-40]

Electrochemical stability is another essential parameter for EC materials. It is well known that in an electrochromic film, the degradation of optical modulation and reversibility is induced by Li^+ ion trapping.[41] Thus, the electrochemical stabilities of as-prepared films were characterized by CA technique using square potentials (between -1.0 and 1.0 V). As shown in Fig. 7. The peak current densities of spray coated film are almost a constant value during 2000 cycles, while that of drop casted film are decreased sharply during 500 cycles, indicating the high stability of the spray coated film. In addition, the spray coated film can stably keep the nanoparticle structure after 2000 cycles, while the nanoparticles turned into dense film after 2000 cycles for the drop casted film (see Fig. S6 in ESI). These results indicate that the spray coated film possesses good cycling durability.

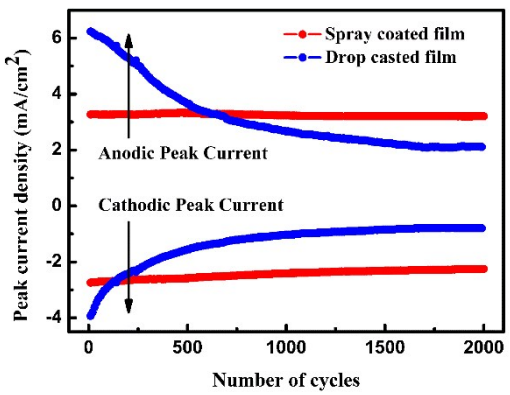

Fig. 7 Peak current evolution of the as-prepared films during the step chronoamperometric cycles.

Conclusions

In summary, a novel and facile method was used to synthesize $W_{0.71}Mo_{0.29}O_{3-x}$ nanoparticles, and an in situ oxidization spray coating technique was utilized to assemble $W_{0.71}Mo_{0.29}O_3$ films. The spray coated $W_{0.71}Mo_{0.29}O_3$ film shows 42.9 % optical contrast at a low voltage, with 10 s coloring and 7.5 s bleaching (to 90%), and coloration efficiency of 36.3 cm^2 C^{-1}. Such spray coated $W_{0.71}Mo_{0.29}O_3$ film demonstrates improved EC behaviors, which possess promising properties for potential applications in energy-saving smart windows and displays. Besides, due to the small size, excellent electrochemical accessibility and the facile film fabrication technique, the thin films of $W_{0.71}Mo_{0.29}O_3$ nanoparticles obtained here hold tremendous promise for nano-electronics, water photo-splitting cells and batteries.

Experimental Section

Synthesis of precursor

All solvents and chemicals were of analytical grade and were used without further purification. The precursor solution was prepared through a modified approach based on our previously reported method.[12,13,30,31] In a typical synthesis route, H_2WO_4 (5 g) and MoO_3 (1.44g) was added to 30 wt % H_2O_2 (60 mL) and heated at 95 °C with stirring. The resulting clear solution was diluted to 200 mL with equal volumes of DI water and EG, giving a concentration of 0.1 M. For comparison, the precursor solution without Molybdenum doping was prepared without adding MoO_3 via the same method.

Synthesis of $WO_3 \cdot 0.33H_2O$ and $W_{0.71}Mo_{0.29}O_{3-x}$

The precursor solution (12 mL) and DI water (12mL) were added into a 40 mL Teflon-lined stainless steel autoclave and maintained at 120 °C for 5 h. After performing the reaction, the products were collected by centrifugation, and thoroughly washed with ethanol and DI water. Then the product was redispersed in DI water to form a pale blue ink for assembly of EC films.

Preparation of EC films

The obtained ink was diluted to 0.5 mg/mL and then drop-casted 30 drops onto an FTO glass covering 8*35 mm^2 area to get a drop casted EC film.

The spray coated film was prepared based on the methods in our previous report.[42] 2.5 mL diluted 0.5 mg/mL ink was deposited onto pre-cleaned FTO glass substrates (2.5*3.5cm^2) by a spray gun in the fume hood. The ink could be dried immediately after being deposited onto the substrates with heating of the hot plate. Meanwhile, the oxygen vacancies could be eliminated due to the in situ heat treatment and a pale yellow EC film could be prepared.

Characterization

X-ray diffraction (XRD, Shimadzu discover diffractometer with Cu Kα-radiation (λ=1.5406 Å)), field-emission scanning electron microscope (FE-SEM, JSM 7600F) and transmission electron microscopy (TEM, JEOL2010) are used to identify the morphology, structure and composition of the products, respectively. The sample roughness was measured using Atomic Force Microscope (AFM) with a Cyphers S (Asylum Research). XPS measurements were performed on a Thermo Scientific K-Alpha spectrometer with a monochromatic Al Kα X-ray source of 1486.6 eV. Ultraviolet-Visible (UV–Vis) spectra were recorded on a UV–Vis spectrophotometer (Shimadzu UV3600). The in situ spectro-electrochemical properties of individual films were carried out in a quartz cell at room temperature in the UV–Vis spectrophotometer, and the voltage supply was from Solartron 1470E. The three-electrode cell consisted of Ag wire as the reference electrode, Pt wire as the counter electrode and the as-synthesized EC film as the working electrode. EIS measurement was conducted by applying an AC voltage of 5 mV over a frequency range of 0.1 Hz to 100 kHz using a Zahner electrochemical workstation (Zennium CIMPS-1). The electrolyte used in this paper was 1 M $LiClO_4$ in PC.

Acknowledgements

We gratefully acknowledge the financial support by Natural Science Foundation of China (No.51172042), Specialized Research Fund for the Doctoral Program of Higher Education (20110075130001), Science and Technology Commission of Shanghai Municipality (13JC1400200), The Shanghai Natural Science Foundation (15ZR1401200), the Program for Professor of Special Appointment (Eastern Scholar) at Shanghai Institutions of Higher Learning, Innovative Research Team in University (IRT1221), the Program of Introducing Talents of Discipline to

Universities (No.111-2-04) and the Fundamental Research Funds for the Central Universities (2232014A3-06). The work is also supported by the Fundamental Research Funds for the Central Universities (15D310604). We are grateful to Nanyang Technological University for supporting the Special Excellent PhD International Visit Program, this work is also partially supported by Donghua University.

Notes and references

[a] *State Key Laboratory for Modification of Chemical Fibers and Polymer Materials, College of Materials Science and Engineering, Donghua University, Shanghai 201620, P. R. China. E-mail: wanghz@dhu.edu.cn; Fax: +86-021-67792855; Tel: +86-021-67792881*

[b] *School of Materials Science and Engineering, Nanyang Technological University, 639798, Singapore. E-mail: pslee@ntu.edu.sg*

[c] *Engineering Research Center of Advanced Glasses Manufacturing Technology, Ministry of Education, College of Materials Science and Engineering, Donghua University, Shanghai 201620, P. R. China. E-mail: yaogang_li@dhu.edu.cn; Fax: +86-021-67792855; Tel: +86-021-67792526*

† Electronic Supplementary Information (ESI) available: [details of any supplementary information available should be included here]. See DOI: 10.1039/b000000x/

‡ Footnotes should appear here. These might include comments relevant to but not central to the matter under discussion, limited experimental and spectral data, and crystallographic data.

1 J. J. Richardson, M. Björnmalm, F. Caruso, *Science*, 2015, **348**, aaa2491.
2 J. Liu, J. Zheng, J. Wang, J. Xu, H. Li and S. Yu, *Nano Lett.*, 2013, **13**, 3589.
3 L. Liang, J. Zhang, Y. Zhou, J. Xie, X. Zhang, M. Guan, B. Pan and Y. Xie, *Sci. Rep.*, 2013, **3**, 1936.
4 S. Cong, Y. Tian, Q. Li, Z. Zhao and F. Geng, *Adv. Mater.*, 2014, **26**, 4260.
5 S. Y. Park, J. M. Lee, C. Noh and S. U. Son, *J. Mater. Chem.*, 2009, **19**, 7959.
6 M. Cui, W. S. Ng, X. Wang, P. Darmawan and P. S. Lee, *Adv. Funct. Mater.*, 2015, **25**, 401.
7 H. Ling, L. Liu, P. S. Lee, D. Mandler and X. Lu, *Electrochim Acta*, 2015, **174**, 57.
8 S. H. Lee, R. Deshpande, P. A. Parilla, K. M. Jones, B. To, A. H. Mahan and A. C. Dillon, *Adv. Mater.*, 2006, **18**, 763.
9 A. Ghicov, S. P. Albu, J. M. Macak and P. Schmuki, *Small*, 2008, **4**, 1063.
10 J. Z. Ou, S. Balendhran, M. R. Field, D. G. McCulloch, A. S. Zoolfakar, R. A. Rani, S. Zhuiykov, A. P. O'Mullane and K. Kalantar-zadeh, *Nanoscale*, 2012, **4**, 5980.
11 J. Zhang, X. L. Wang, X. H. Xia, C. D. Gu, Z. J. Zhao and J. P. Tu, *Electrochim Acta*, 2010, **55**, 6953.
12 H. Li, G. Shi, H. Wang, Q. Zhang and Y. Li, *J. Mater. Chem. A*, 2014, **2**, 11305.
13 H. Li, J. Wang, G. Shi, H. Wang, Q. Zhang and Y. Li, *RSC Adv.*, 2015, **5**, 196.
14 D. Ma, G. Shi, H. Wang, Q. Zhang and Y. Li, *J. Mater. Chem. A*, 2014, **2**, 13541.
15 W. Kang, C. Yan, X. Wang, C.Y. Foo, A. W. M. Tan, K. J. Z. Chee and P. S. Lee, *J. Mater. Chem. C*, 2014, **2**, 4727.
16 Y. Lu, L. Liu, W. Foo, S. Magdassi, D. Mandlerb and P. S. Lee, *J. Mater. Chem. C*, 2013, **1**, 3651.
17 M. Wong, R. Ishige, K. L. White, P. Li, D. Kim, R. Krishnamoorti, R. Gunther, T. Higuchi, H. Jinnai, A. Takahara, R. Nishimura and H. J. Sue, *Nat. Commun.*, 2014, **5**, 3589.
18 J. H. Lee, S. Yoshikawa and T. Sagawa, *Sol. Energy Mater. Sol. Cells*, 2014, **127**, 111.
19 Y. Lin, T. Tsai, S. Hung and S. Tien, *J. Solid State Electrochem.*, 2013, **17**, 1077.
20 K. A. Gesheva and T. Ivanova, *Chem. Vap. Deposition*, 2006, **12**, 231.
21 L. Kondrachova, B. P. Hahn, G. Vijayaraghavan, R. D. Williams and K. J. Stevenson, *Langmuir*, 2006, **22**, 10490.
22 K. A. Gesheva, A. Cziraki, T. Ivanova, A. Szekeres, *Thin Solid Films*, 2007, **515**, 4609.
23 J. M. O. R. de León, D. R. Acosta, U. Pal and L. Castaneda, *Electrochim. Acta*, 2011, **56**, 2599.
24 L. M. Manceriu, A. Rougier and A. Duta, *J. Alloy. Compd.*, 2015, **630**, 133.
25 H. Zheng, J. Z. Ou, M. S. Strano, R. B. Kaner, A. Mitchell and K. Kalantar-zadeh, *Adv. Funct. Mater.*, 2011, **21**, 2175.
26 H. Cheng, T. Kamegawa, K. Mori and H. Yamashita, *Angew. Chem. Int. Ed.*, 2014, **53**, 2910.
27 K. Manthiram and A. P. Alivisatos, *J. Am. Chem. Soc.*, 2012, **134**, 3995.
28 G. Song, J. Shen, F. Jiang, R. Hu, W. Li, L. An, R. Zou, Z. Chen, Z. Qin and J. Hu, *ACS Appl. Mater. Interfaces*, 2014, **6**, 3915.
29 B. Dasgupta, Y. Ren, L. M. Wong, L. Kong, E. S. Tok, W. K. Chim and S. Y. Chiam, *J. Phys. Chem. C*, 2015, **119**, 10592.
30 D. Ma, G. Shi, H. Wang, Q. Zhang and Y. Li, *J. Mater. Chem. A*, 2013, **1**, 684.
31 D. Ma, H. Wang, Q. Zhang and Y. Li, *J. Mater. Chem.*, 2012, **22**, 16633.
32 S. Vankova, S. Zanarini, J. Amici, F. Cámara, R. Arletti, S. Bodoardo and N. Penazzia, *Nanoscale*, 2015, **7**, 7174.
33 F. Zheng, H. Lu, M. Guo and M. Zhang, *CrystEngComm*, 2013, **15**, 5828.
34 D. D. Yao, R. A. Rani, A. P. O'Mullane, K. Kalantar-zadeh and J. Z. Ou, *J. Phys. Chem. C*, 2014, **118**, 476.
35 B. N. Reddy, P. N. Kumar and M. Deepa, *ChemPhysChem*, 2015, **16**, 377.
36 C. Zhao, F. Du and J. Wang, *RSC Adv.*, 2015, **5**, 38706.
37 W. Xiao, W. Liu, X. Mao, H. Zhu and D. Wang, *J. Mater. Chem. A*, 2013, **1**, 1261.
38 J. Wang, E. Khoo, P. S. Lee and J. Ma, *J. Phys. Chem. C*, 2009, **113**, 9655.
39 J. M. Wang, E. Khoo, P. S. Lee and J. Ma, *J. Phys. Chem. C*, 2008, **112**, 14306.
40 N. M. Vuong, D. Kim and H. Kim, *J. Mater. Chem. C*, 2013, **1**, 3399.
41 R. T. Wen, C. G. Granqvist and G. A. Niklasson, *Nat. Mater.*, 2015, 14, 996.
42 J. Wang, C. Yan, W. Kang and P. S. Lee, *Nanoscale*, 2014, **6**, 10734.

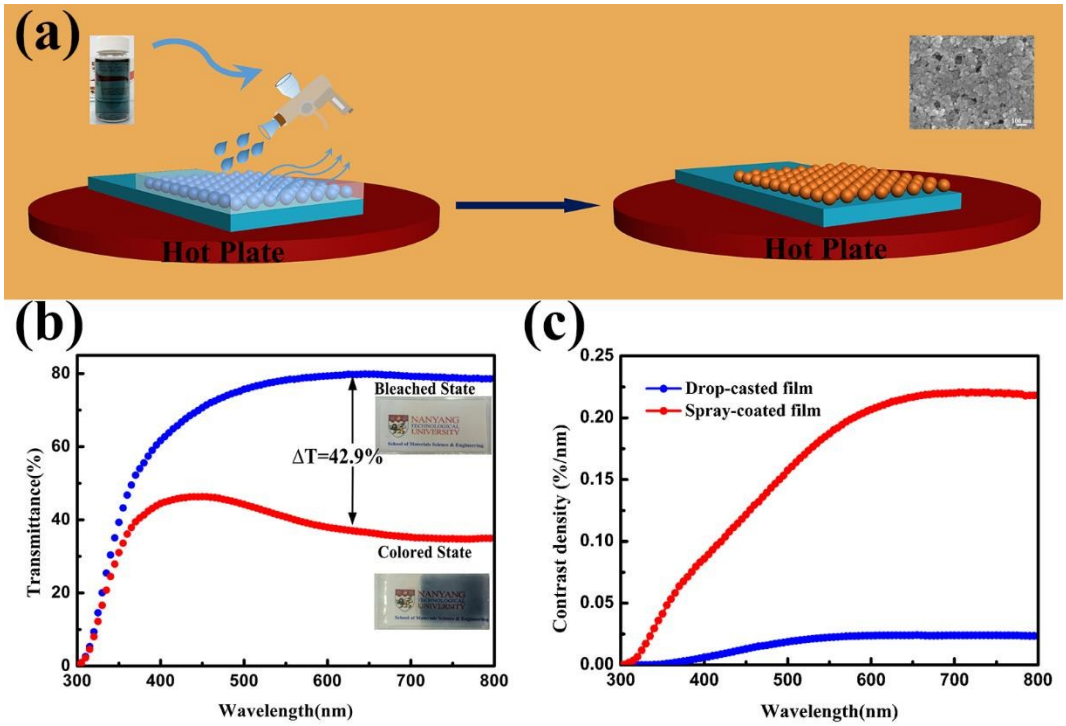

Crystal defects induced by molybdenum doping is utilized to synthesize aqueous tungsten molybdenum oxide nanoparticle ink and enhanced electrochromism is obtained with spray coating technique.